AS SEEN IN
JULY 2014 E&P

Microseismic correlation to production – A Horn River completions evaluation case study

Asal Rahimi-Zeynal, **Mike Mueller** and
Sudhendu Kashikar, MicroSeismic Inc.

Microseismic is now an accepted technology used to monitor hydraulic fracturing that measures the geometry, location and complexity of the fractures. Although microseismic monitoring has added value in understanding hydraulic fractures, there is still significant information and value that can be extracted from many microseismic monitoring programs. Most of the microseismic analysis performed to date is qualitative and has provided limited value in optimizing completions.

To fully optimize the completion and fracture treatment, it is important to understand various aspects of fracturing treatment such as differentiating propped and unpropped fractures, fracture growth and geometry, fracture overlap between stages and wells, stress shadowing effects and treatment efficiency. Currently this is achieved by a qualitative comparison of microseismic points with simulation models.

Figure 1 shows an idealized process for completions and fracture optimization. Today, fracture evaluation is performed using various simulations that may use as input microseismic pointsets to qualitatively calibrate the model. New developments enable valuable information to be extracted by combining contextual information such as geology, well logs, treatment data, etc., with deterministic analysis of the microseismic measurements. The result of this deterministic analysis provides quantification of the hydraulic fracturing. Some of the key aspects of this analysis are:

- Fracture geometry—height, length and azimuth;
- Fracture complexity and tortuosity;
- Fracture coverage (overlap between stages and wells);
- Characterization of fracture mechanisms (dip-slip, strike-slip, etc.); and
- Identification and avoidance of geohazards.

The completions evaluation analysis provides a mechanism to better calibrate and build underlying geomechanical and reservoir models, improving forecasting of fracture placement and production and helping to accelerate optimization of future wells and treatment designs.

This distinct process of completions evaluation consists of a workflow and tools to perform diagnostic analysis of microseismic pointsets, enabling accurate evaluation of the fracture treatment. It is designed to precisely characterize the fracture network growth and complexity while providing a methodology to evaluate the wellbore spacing, stage lengths, cluster spacing and treatment parameters.

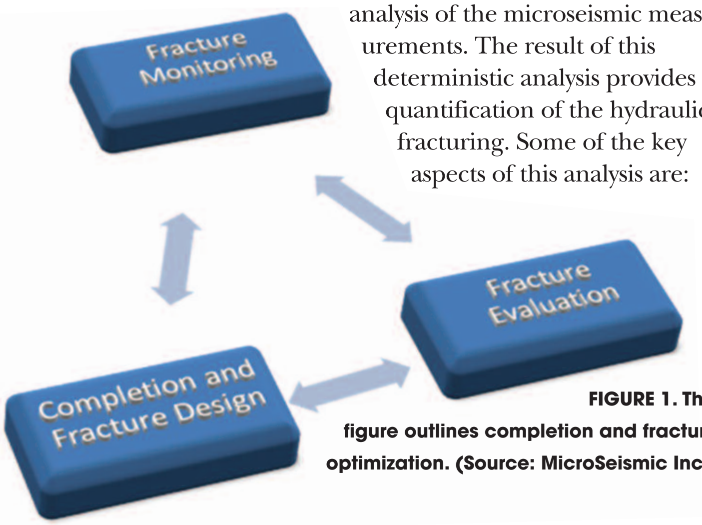

FIGURE 1. This figure outlines completion and fracture optimization. (Source: MicroSeismic Inc.)

Case study

In a field located in northeast British Columbia in the Horn River Basin, the target is the Muskwa and Evie members of the Horn River Formation. Gas is produced from both members, but commercial production requires horizontal drilling and fracturing since it is low-permeability. Original gas-in-place estimates in the Horn River are in excess of 14.2 Tcm (500 Tcf), making this the third-largest undeveloped gas resource in North America.

The microseismic acquisition method used a permanently installed near-surface buried array consisting of 98 stations (Figure 2). The wide-azimuth, large-aperture and high-fold geometry allows for a consistent microseismic event resolution under the entire footprint of the array, in this case covering an area of more than 40 sq km (15.4 sq miles). This acquisition geometry provides rich wavefield sampling and enables high-quality passive seismic emission tomography imaging, resulting in a high-confidence estimate of event magnitude and determination of the failure mechanism for every event.

The location of this case study was at a seven-well pad in the Horn River Basin in which 201 fracture stages over a

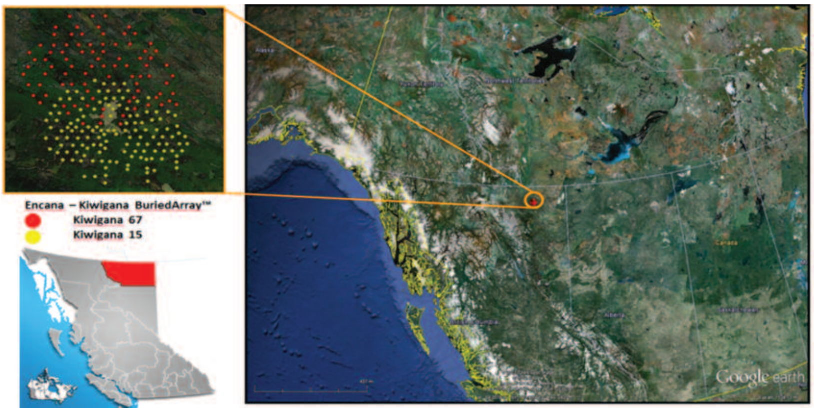

FIGURE 2. Almost 100 near-surface arrays were used in the Encana survey. (Source: MicroSeismic Inc.)

70-day period were monitored. Figure 3 shows the wells displayed with green color. Pink dots represent microseismic events resulting from the stimulation job. During the monitoring period, more than 11,200 events were detected and located. The events are mostly confined to the target zones. Hypocenter event location uncertainty is on the order of 10 m (30 ft) laterally and 20 m (60 ft) vertically as determined from velocity calibration using perforations and the event signal-to-noise ratio.

Modeling the microseismic events as 3-D fractures allows the computation of fracture flow properties by assigning various attributes to the modeled fracture planes. This is based on the assumption that the microseismic events indicate rock failure. This modeling based on a microseismic pointset creates a discrete fracture network (DFN, Figure 4).

The DFN was generated using event attributes from the microseismic pointset. In the modeling approach every fracture plane is centered on a microseismic event. For each event the source mechanism was identified and the failure orientation for each fracture plane was assigned according to the source mechanism. Fracture lengths are calculated from the seismic moment of each event.

The positioning and overall geometry of the modeled DFN and individual fracture set strikes and dips provides insights into the stimulation effectiveness, drainage patterns, unstimulated zones and influence of geologic features such as geohazards.

There is consistent fracturing to the west of the pad, more intense formation response to the stimulation in the east and a possibly unstimulated area along and immediately west of a larger swarm of strike-slip events. These features may be interpreted more confidently due to the laterally large acquisition footprint, which allows equal and consistent microseismic imaging across and beyond the entire pad.

When the DFN model is placed in a geocellular framework, the total fracture volume, average fracture aperture and total stimulated reservoir volume (SRV) may be calculated. The SRV is defined as the sum of the volume of all of the cells in the geocellular model for which nonzero values are calculated. The cell size in the model is 30 m (90 ft) on each side. Relative fracture permeability is calculated for every cell in the model that contains a fracture, including partial fractures.

The SRV characterizes the volume of reservoir rock with increased permeability due to stimulated fractures (Figure 5).

Microseismic-based well productivity estimates are based on the assumption that in ultralow-permeability shale reservoirs, pore pressure changes due to hydraulic fracturing cannot move far away from the activated fractures. Therefore, the microseismic event cloud or pointset corresponds to the effective fracture network size. The 3-D volume of the microseismic pointset can be estimated as the maximum extent of the stimulated fracture network. While the effectively producing fracture network could be smaller by a certain percentage, it is expected that the effective network and the stimulated network have a direct correlation. However, SRV is not the only driver of well production. In a given SRV, fracture conductivity and fracture spacing can affect hydrocarbon production and can have a major impact in recovery calculations.

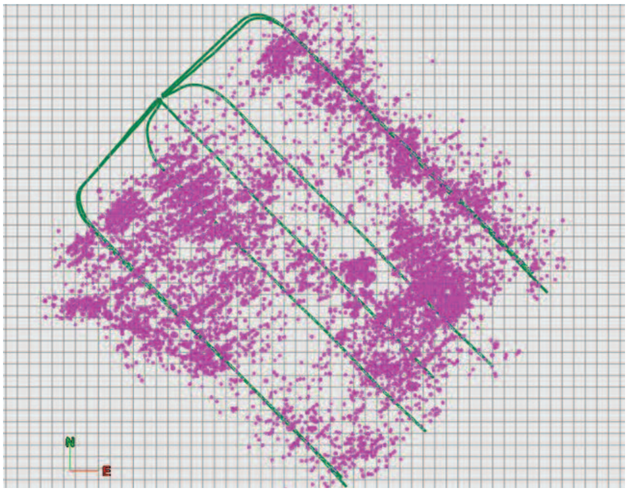

FIGURE 3. Wells are displayed in green. Pink dots represent microseismic events resulting from the stimulation job. (Source: MicroSeismic Inc.)

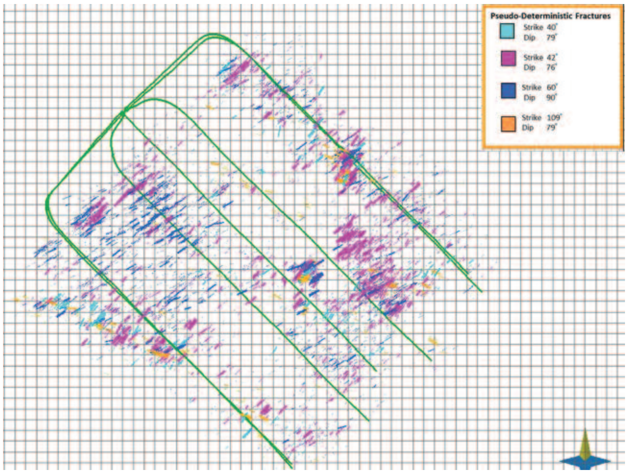

FIGURE 4. This map view shows the DFN. (Source: MicroSeismic Inc.)

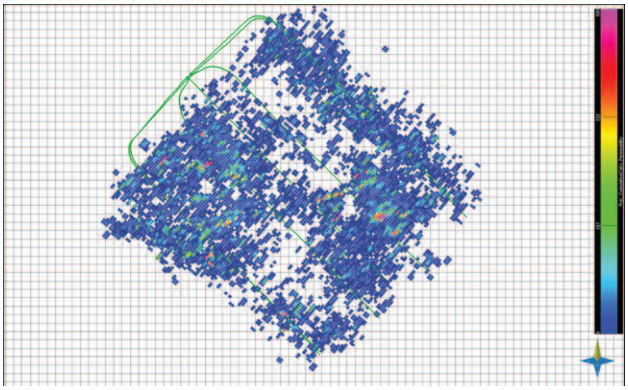

FIGURE 5. In this map view of the modeled SRV calculated from DFN, the color bar shows relative fracture permeability. (Source: MicroSeismic Inc.)

Results

The individual well SRVs obtained from the microseismic pointset are compared with actual field 30-day production data. This demonstrates the correlation of the microseismic results with production from the seven-well pad. Testing is underway to determine whether this concept may be used to predict well performance. The plot shows that larger SRVs result in higher well production for the Horn River Basin study wells (Figure 6). Deviations from the linear relationship might be related to variations in geology (i.e., reservoir quality) as well as fracture spacing and conductivity. This plot does not provide a deterministic quantification of what percentage of the network is contributing to production.

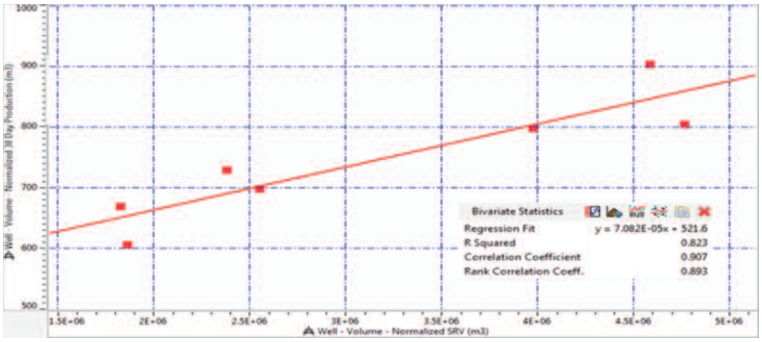

FIGURE 6. The correlation of SRV to production is shown in the Horn River Field. (Source: MicroSeismic Inc.)

The quantification of the effective size of the fracture network may be performed by numerical reservoir simulators and proppant placement analysis. For this study, the 90% correlation of the well-by-well total SRV vs. 30-day production data demonstrates that this concept may be used to predict microseismic-based well productivity.

The 90% correlation between production and SRV for each well shows that larger SRVs result in higher well production regardless of the percentage of the SRV that contains proppant-filled fractures for the first 30 days. The direct relationship of the SRV and production can be used to predict a new well's potential productivity immediately upon completion of the stimulation job. This suggests that a key completion effectiveness tool is to provide production prediction by monitoring stimulation microseismically. This may allow operators to optimize their overall completions planning and, in turn, maximize recovery.

Extensive microseismic results across the top shale oil and gas plays in the U.S. and Canada have been gathered and used to understand the correlation of microseismicity to production at the local scale. From this analysis the relationship between microseismic pointsets and hydrocarbon production was determined. This can be used to predict a new well's potential productivity immediately upon completion of the stimulation job.

Operators may test varying completion techniques to determine which treatment design gives the largest and most effective SRV and use this information to obtain maximum recovery and well performance. E&P

Acknowledgments

The authors acknowledge MicroSeismic Inc., Encana Corp. and Kogas Canada for contributing data and for supporting this research. Special thanks to Michael de Groot for his assistance. Some of this information appeared in SPE paper 169541 and has been reprinted with permission.